IOP Conf. Series: Materials Science and Engineering **364** (2018) 012096 doi:10.1088/1757-899X/364/1/012096

THz imaging tool for characterizing both visible and concealed metals in paint layers

I. Cacciari[1], D. Ciofini[1], L. Gallo[2], S. Siano[1]

[1]Istituto di Fisica Applicata "Nello Carrara", Consiglio Nazionale delle Ricerche, v. M. del Piano 10, 50019 Sesto Fiorentino (FI), Italy

[2]Gallo Restauro, v. S. Zanobi 104/R, 50129, Florence, Italy

i.cacciari@ifac.cnr.it

Abstract. The Terahertz (THz) radiation can penetrate optically opaque materials, and in combination with low photon energy makes possible imaging applications in a variety of fields such as biomedicine, material science, security, etc.. This has motivated a growing interest in THz techniques during recent years and, in turn, has resulted in significant technological improvements and the introduction of several commercial-type systems. In particular, THz technology has been demonstrated to be particularly useful for the study of multi-layered non-metallic structures such as those encountered in easel and mural paintings, as well as of glued paper layers and of other similar ones. This work focuses on metallic layers concealed beneath paint layers in which THz imaging can be very effective thanks to the high reflection of metals. THz imaging measurements have been carried out using a time-domain THz spectrometer equipped with an XY translation stage. Both mock-ups and original multilayer samples were imaged. The former were prepared by gluing metal foil polygonal shapes onto a plastic substrate and then covering the whole of it with paint layers. The THz imaging revealed the metal shape beneath the paint layers, thus making possible some assessments on the layer depth. Original pictorial samples from a Sienese painting of the XIII-XIV century were also investigated. In this particular case, the THz imaging was capable of distinguishing between the original gold leaf and the paint layers (overpaint).

1. Introduction

The spectral region between 0.1 and 3 THz is commonly referred to as the Terahertz (THz) region. Its application for spectroscopy and imaging in the field of the cultural heritage has witnessed a growing interest that has generated research into a variety of new applications [1-9].

The THz wave has attracted particular interest within the field of the cultural heritage as it is completely safe being non-ionizing, and non-destructive since there is no contact with the artwork. It can also penetrate a wide variety of dielectric materials (*e.g.* stone, fabric, paper, plastic, leather, wood, and many others) and make it possible to "see" through opaque materials that are generally used in the fabrication of culturally valuable objects (such as stone, paper manuscript, wood, and many others).

In the case of a dielectric slab, due to the index change, the incident THz beam is partly reflected at the front air/surface interface, thus leading to a first reflected signal. The remaining part of the signal

propagating through the sample thickness experiences a further partial reflection at the back of the sample, thus leading to a temporally-separated echo (second reflection). In the case of a multilayer sample, other reflections occur since there are other interfaces within the sample thickness.

In general, for each point of the sample under investigation, THz imaging records the amplitude of each reflected pulse and creates the corresponding false colour images. This approach is found to be extremely interesting, because the amplitude of the reflections is mostly determined by the material absorption and the surface smoothness, and hence, considerable information can be obtained. However, when the signal reflected is comparable to the system noise, i.e. when a high value of absorption characterizes the material, the imaging does not provide useful information. On the contrary, with metal surfaces, the THz pulse is totally reflected and there are no other subsequent reflections. We find this case extremely intriguing, due to the fact that the absorption does not have a role in providing information on layer thickness. In this regard, we focused our work on imaging multilayer samples made of visible and concealed metal. The THz setup described in section 2 have been used to image mock-ups in which the metal layers were concealed and original painting in which the metal layers were partially visible. The results of these measurements have been discussed in section 3 and, lastly, section 4 contains the conclusions drawn.

2. Materials and methods

2.1.1. THz imaging setup.

A THz time-domain spectrometer equipped with emitter and receiver in reflection geometry was used [10] for the refractive index and imaging measurements. This setup was chosen because it makes possible spectroscopic studies on multi-layered paint samples, i.e. samples which cannot be easily measured in transmission geometry. The incident and collection angles were placed at 30° to the normal sample surface. The THz pulse was emitted by illuminating a photoconductive antenna (PCA Emitter) with an ultrafast pulse (70 fs) from a fibre Erbium Laser (Toptica, Femto-FErb 1560) emitting at 1550 nm. The ultrafast pulse was then split into two guided beams: one was used for the generation and the other, for detection. A series of mirrors and lenses guided the ultrafast pulse to the emitter, which was coupled to a single mode fibre with a FC/PC connector for supplying the ultrafast pulse. The THz pulse emitted by the PCA was collimated and focused with plastic lenses on the sample, and the reflected signal from the sample was focused back by using a second pair of lenses on the detector (PCA Detector). The THz time domain spectrometer is schematically presented in figure 1.

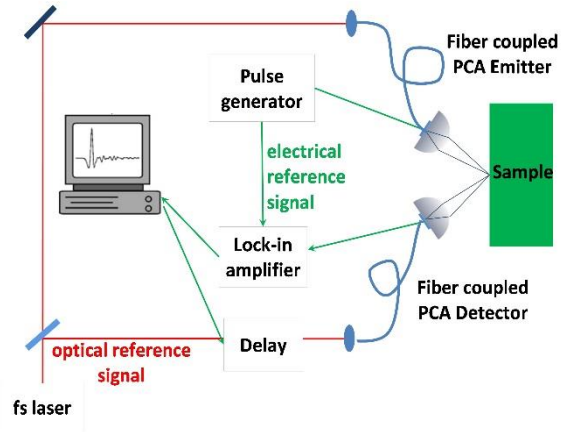

Figure 1. THz imaging setup.

In order to vary the arrival time of the signal with respect to the pulse used for detection, a delay stage was introduced into the generation arm. By scanning the delay line, both the electric field amplitude (A) and the phase of the THz waveform could be sampled as a function of time. A LabVIEW® software saved the electric field amplitude from a digital lock-in amplifier that measured the signal from the detector using a data acquisition card from National Instruments®. The bandwidth obtained with this setup ranged from 0.1 to 2.5 THz. In the present work, both the emitter and detector in reflection geometry were fastened on a two-axis translation stage that represents the only moving part of the imaging setup. The translation stage could move in a plane parallel to the sample surface. The THz image of a sample was taken by moving the stage in the x-y plane (the z axis is defined as the normal surface direction). The step sizes were 1 mm along both the x and y axes. Full THz temporal waveforms were recorded for each emitter-detector position, and the difference between the maximum and minimum amplitude for each reflected pulse was considered to form the corresponding THz image.

2.1.2. Samples

With the aim of exploring the penetrating properties of THz radiation in optically opaque artistic materials, purpose-designed laboratory samples reproducing a multi-layered stratigraphy were prepared and systematically investigated. A representative drawing illustrating the stratigraphic sequence of the two different types of prepared samples (samples A and B) is shown in figure 2. The first operative step, for both samples A and B, was that of creating rounded copper foils. For this purpose, 100 μm thick copper foils were first hole punched using a round metal tip of 8 mm diameter and were then glued onto the back side of Corning™ Falcon™ Petri Dishes. The latter consisted of crystal-grade polystyrene (PS), had a 35 mm diameter, an 11.8 cm² area and 500 μm of indentation which made it possible to exploit it as a mould for the final application of the paint coating. As shown in figure 1, three non-superimposed copper foils were applied for sample A, whereas a vertical stack of two and three copper foils were added to sample B. Paint coatings were then formulated using a mixture of pigment powder dispersed in a binding medium. The pigment selected was a commercial variety of synthetic cobalt blue (purchased from Zecchi, Florence), a cobalt aluminium oxide ($CoAl_2O_4$) manufactured in Europe in 1802 that was used from ancient times up to the nineteenth century as an artistic pigment for producing paints for decorating ceramic glazes and jewellery [11]. In particular, the choice was further motivated by the findings obtained in a previous work [12], in which cobalt blue, among the pigments studied, showed a relatively high refractive index and a significant THz reflection.

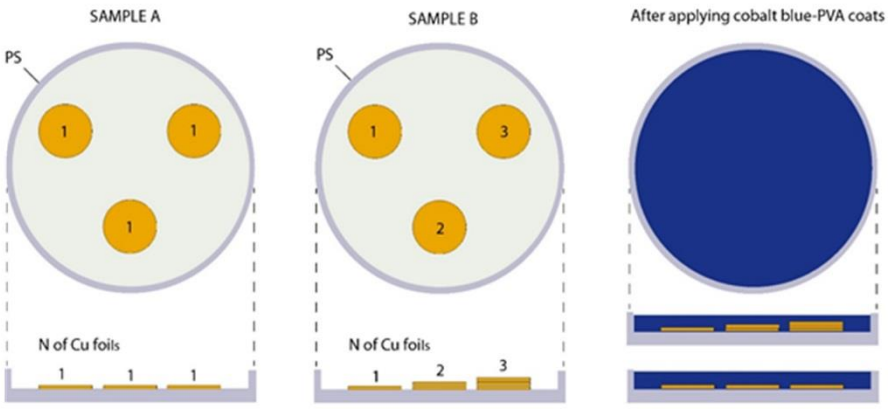

Figure 2. Multilayer Mockups preparation.

Figure 3. THz antennas analysing original pictorial sample. The box corresponds to the THz imaging area.

Figure 4. THz imaging area.

The pigment powder was finely ground, added in a 1:1 ratio to a 10 % (w/v) polyvinyl-alcohol (PVA)-water solution, and then thoroughly blended. PVA was selected because of its superior dispersing properties. Thus, after gluing the copper foils onto a PS substrate, the cobalt blue-PVA mixture was spread out so that it covered the PS mould with the three round copper foils. Usually, additional coats of paints were needed in order to fill the PS mould completely and to conceal the three copper sheets. After applying the cobalt blue-PVA coatings (third step of figure 2), samples A and B were left to be cured under laboratory conditions (23 ± 1 °C and 50% HR) for 7 days and were then analysed.

Moreover, an original pictorial sample from a Sienese painting of the XIII-XIV century was also investigated. In this sample, the gilding was performed by applying gold leaf to a red bole layer, in figure 3 is shown the THz antenna during the measurements and in figure the area considered for the imaging.

3. Results and discussion

Samples A and B were imaged using the THz setup shown in figure 1. For each pixel, two pulses could be observed: the first peak came from the air/painting interface; the second came from the painting/metal or from painting/polystyrene interfaces. The amplitude of the first peak (for all the pixels considered in samples A and B) is presented in figure 5 and 6.

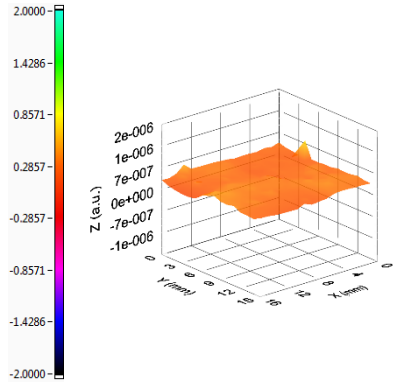

Figure 5. Amplitudes of the first peaks of sample A. The vertical scale is expressed in a.u., while the factor 10^{-6} is omitted for simplicity.

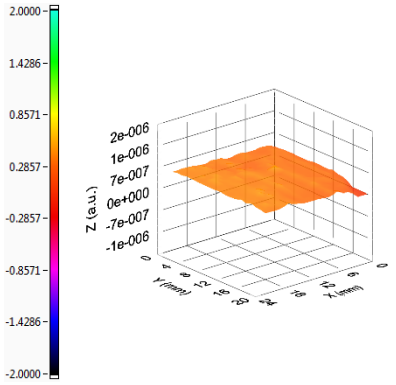

Figure 6. Amplitudes of the first peaks of sample B. The vertical scale is expressed in a.u., while the factor 10^{-6} is omitted simplicity.

We considered a 3D representation of these data in order to point out that the sample surface was smooth and the optical axis was normal for the surface. The first observation could be drawn by calculating the mean value of the amplitudes: we obtained $3.01 \times 10^{-7} \pm 10\%$ a.u. and $3.4 \times 10^{-7} \pm 10\%$ a.u. for samples A and B, respectively. The error associated was calculated as the standard deviation. On a rough surface the first peak amplitude is likely to be attenuated [10], and in general the corresponding standard deviation is more than 10%. Moreover, this observation is corroborated by the orthogonal position of the sample surface to the optical axis. In the case of a tilted sample surface, there are points closer and further away, and this determines an attenuation of the corresponding amplitudes that leads to a standard deviation of more than 10%.

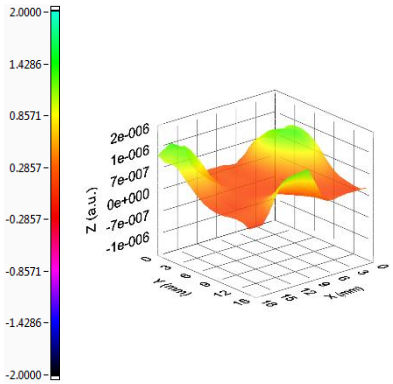

Figure 7. Amplitudes of the second peaks of sample A. The vertical scale is expressed in a.u., while the factor 10^{-6} is omitted for the sake of brevity.

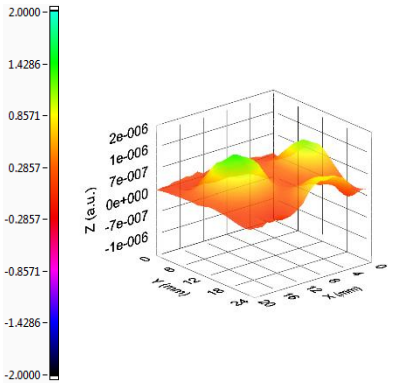

Figure 8. Amplitudes of the second peaks of sample B. The vertical scale is expressed in a.u., while the factor 10^{-6} is omitted for the sake of brevity.

The amplitudes of the second peak of samples A and B have been represented, respectively, in figures 7 and 8. The imaging clearly illustrates that, beneath the first absorbing layer, there are layers of highly reflective material (in this case, metal foil) that are round in shape. Where the amplitude is greater, there is a painting/metal interface and no more pulses can be evidenced because the metal foil blocks any further reflections. On the contrary, where the amplitude is less, the signal is absorbed by the paint layer and another reflection (the third) is due to the painting/polystyrene interface. It is interesting to note that, in the case of sample A (figure 7), the amplitudes of the THz signals reflected at the metal foils are almost the same: 1.31×10^{-6}, 1.30×10^{-6} and 1.29×10^{-6} a.u.. In this case, the THz signal travelled the same thickness of paint layer before reflecting the metal foil. It therefore underwent the same degree of attenuation. This was not true for sample B: the reflections at the metal foils (figure 8) were different. In correspondence with these points we obtained maximum amplitudes of 1.37×10^{-6}, 1.15×10^{-6} and 0.88×10^{-6} a.u.. This was compatible with the way in which the sample was prepared. In fact, the three metal foils were covered by different thicknesses of paint, the signal reflected by one metal foil was more attenuated because it travelled a greater thickness of paint. On the contrary, where it travelled a lesser thickness, the attenuation was lower. The corresponding paint thicknesses could be calculated by considering the dish indentation and the metal foil thickness: we obtained 200 μm, 300 and 400 μm. It was possible to establish a linear fit between the thickness of the paint layers and the maximum amplitudes in correspondence with the metal foils the goodness of this relationship was determined by a R^2 of 0.99. It should be noted that, the metal foil thickness prevents the THz pulse to penetrate into the metal, thus the glue used in the two mockups does not interfere with the measurements and in particular with the pulse attenuation.

In the case of original pictorial gilded samples, in which the gilding was performed by applying gold leaf to a red bole layer (figure 4), the potential of THz imaging appeared to be even more evident.

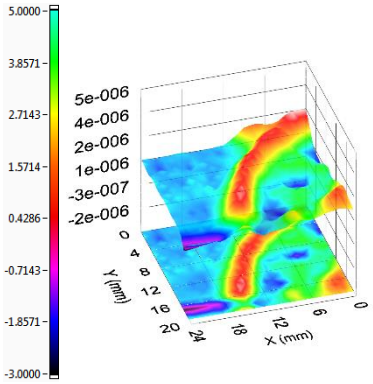

Figure 9. THz imaging of figure 4.

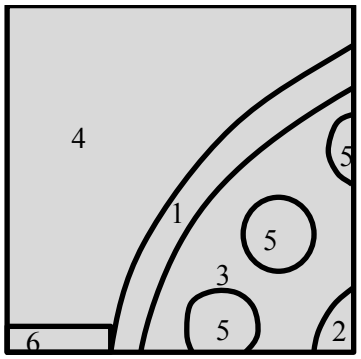

Figure 10. Different areas in terms of amplitude evidenced by THz imaging.

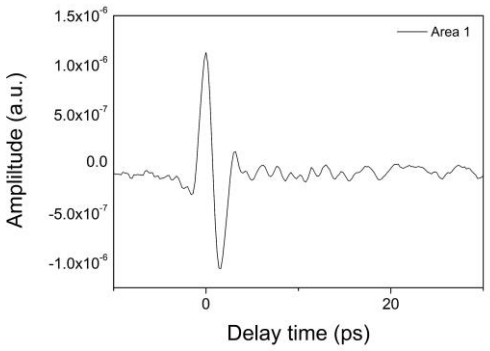

Figure 11. THz pulse reflected from area 1.

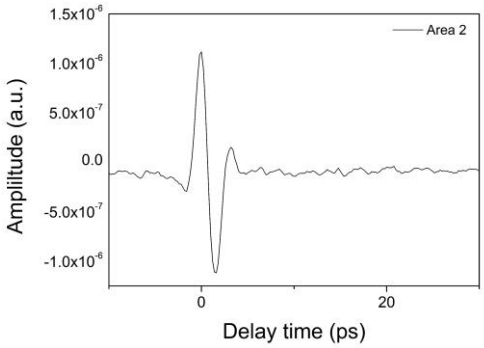

Figure 12. THz pulse reflected from area 2.

The THz imaging is shown in figure 9. Several areas, characterized by different amplitude values, have been highlighted and, for the sake of clarity, have been sketched in figure 10: in ascending order, these are areas 1 and 2 (~$2x10^{-6}$ a.u.), areas 3 and 4 (~$1x10^{-6}$ a.u.), and lastly areas 5 and 6 (~$0.8x10^{-6}$ a.u.). The greater amplitudes of areas 1 and 2 of figure 9 could have been due to the reflection at a metal interface (gold leaf). This was confirmed by observing the corresponding THz signals (figures 11 and 12): only the first peak (due to the reflection at air/metal interface) existed. Moreover, it is worth noting that, in the original image (figure 4), the gold leaf is visible while, on the contrary, in areas 3 and 4 the gold leaf has been partially lost and the red bole is fairly observable. In terms of THz imaging, this led to an absorption of the THz pulse while traveling the red bole and, therefore, a lower amplitude than in areas 1 and 2 is appreciable in both areas 3 and 4.

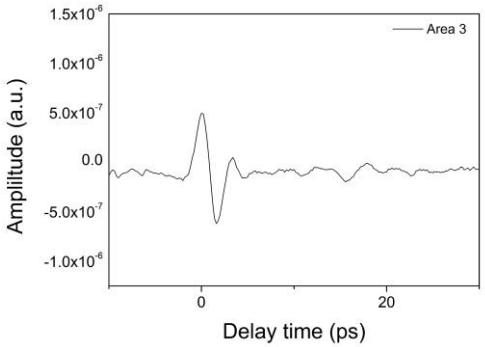

Figure 13. THz pulse reflected from area 3.

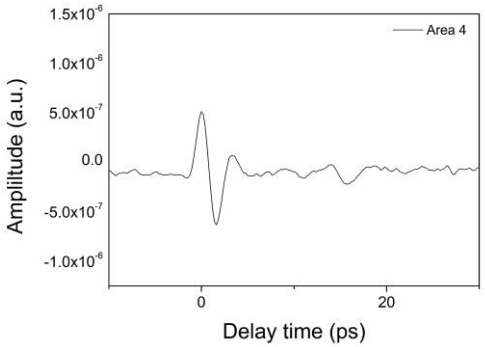

Figure 14. THz pulse reflected from area 4.

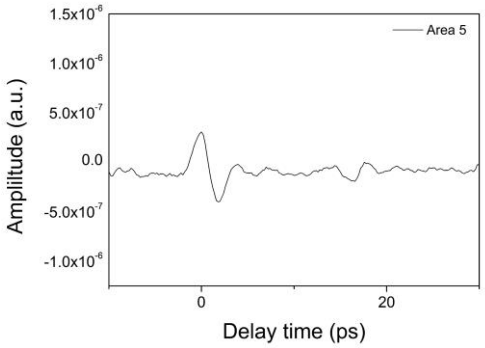

Figure 15. THz pulse reflected from area 5.

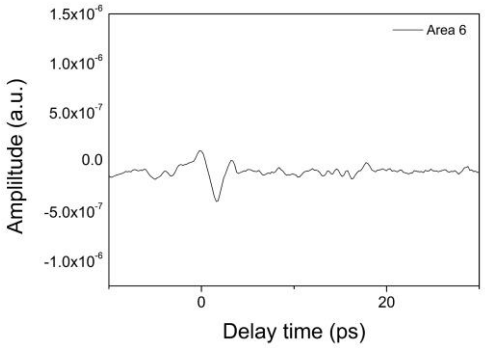

Figure 16. THz pulse reflected from area 6.

Moreover, the corresponding THz signals (figures 13 and 14) reveal the presence of a second pulse reflection, which is due to the red bole/preparation interface. Areas 5 and 6, which correspond to the punch work [13], are also extremely interesting. They are similar to areas 3 and 4, but show lesser amplitudes (figure 15). This may be due to the punch work itself: in that case, the surface is more distant than the previous areas from the emitter and the detector. This means that the incident THz pulse is not in the focal plane when it arrives on the surface, and that an absorption and possibly a small broadening could be affecting the propagation. This is accentuated in area 6, where the lesser amplitude (figure 16) is due to the horizontal craquelure.

4. Conclusions

This paper shows the feasibility of using THz imaging in the field of the characterization of artworks. A THz time-domain spectrometer was equipped to perform imaging measurements. This setup has been used to image samples that presented concealed or visible metal interfaces. In the first case, laboratory samples were prepared in order to study, starting from THz imaging, the layer stratigraphy. In particular, some considerations on the painting surface and layer thickness have been made by measuring the peak amplitudes of the THz pulse reflected at the air/pigment and pigment/metal interface. In the case of a

visible metal interface, we imaged a portion of an original painting in which the metal is presented as a gold leaf on a red bole layer. The THz imaging distinguished the areas in which the metal is not lost from the areas in which the red bole or possibly an overpainting are present. This may be of great importance in the field of authentication.

5. Acknowledgements

The present work was carried out within the IPERION CH (H2020-INFRAIA-2014-2015, Grant No. 654028) project. The authors also acknowledge the financial support of the "Fondo per le infrastrutture produttive" of the Tuscan Region (D.G.R.T. n. 924 - 19/10/2009), for the purchase of the THz time-domain spectrometer used in the present study.

6. References

[1] Fukunaga K, Ogawa Y, Hayashi S and Hosako I 2007 *IEICE Electronics Express* **4** 258-263.
[2] Jackson J B, Mourou M, Whitaker J F, Duling I N, Williamson S L Menu M, Mourou G A 2008 *Opt.* Comm. **281** 527-532.
[3] Jackson J B, Bowen J, Walker G, Labaune J, Mourou G, Menu M and Fukunaga K 2011 *IEEE Trans. Terahertz Sci. Technol.* **1** 220-231.
[4] Jepsen P U, Cooke D G and Koch M 2011 *Laser & Photonics Reviews* **5** 124-166.
[5] Walker G C, Labaune J, Bowen J W, Jackson J, Hadjiloucas S, Mourou G, Menu M 2011 *36th International Conference on Infrared, Millimeter and Terahertz Waves (IRMMW-THz)* 1-2.
[6] Picollo M, Fukunaga K, Labaune J 2015 *J. Cult. Herit.* 2015 **16** 73-80.
[7] Dong J, Jackson J B, Melis M, Giovanacci D, Walker G C, Locquet A, Bowen J W and Citrin D S 2016 *Opt. Express* **24** 26972-26985.
[8] Cacciari I, Agresti J, Siano S 2016 *Microchem. J.* **126** 76-82.
[9] Zhang H, Sfarra S, Saluja K, Peeters J, Fleuret J, Duan Y, Fernandes H, Avdelidis N, Ibarra-Castanedo C, Maldague X 2017 *J Nondestruc Eval* **36** 1-12.
[10] Cacciari I, Siano S 2017 *J Infrared Milli Terahz Waves* **38** 503-517.
[11] Gettens R J, Stout G L, *Painting Materials: A Short Encyclopaedia* 1966 (Dover Publications).
[12] Cacciari I, Ciofini D, Siano S 2015 *IET Conf. Publ.* 1-4.
[13] Cacciari I, Nieri P, Siano S 2014 *J. Comput. Cult. Heritage* **7** 1-14